Charge-state dependence of fluorine K x rays in F-Ne collisions

Philip L. Pepmiller and Patrick Richard
Department of Physics, Kansas State University, Manhattan, Kansas 66506
(Received 26 February 1982)

The K x-ray-production cross sections for fluorine are measured as a function of charge state for 15-MeV $F^{q+}+Ne$ collisions. The measurements are differential in energy of the K x rays with sufficient resolution to identify the final-state configurations of the fluorine ions following the collision. The final states are identified with the processes of single K-shell to L-shell excitation, single K-shell—multiple L-shell ionization, and single L-shell electron capture.

I. INTRODUCTION

In the last few years measurements of the K x-ray spectra of energetic ions incident on gas targets have been used to study the relative importance of the different excitation mechanisms in ion-atom collisions.[1-4] The x-ray transitions observed in high resolution can be related to the atomic state formed in the collision, which in turn can be related to the vacancy-production mechanism when single-collision conditions are maintained. The charge-state dependence of the K-shell excitation and K-shell ionization cross sections have been measured by this technique for 15-MeV $F^{q+}+He$ collisions.[4] It was found for this asymmetric collision system that the F K-shell excitation cross section increased dramatically with increase in projectile charge state and that the ionization cross section decreased with increase in projectile charge state. The ratio of the excitation to ionization cross sections varied from 0.1 to 4.0 for projectile charge states 2^+ to 6^+. The relative importance of electron capture was also determined for projectiles with K-shell vacancies by observing the K x rays identified with capture to excited states. For one-electron projectiles (F^{8+}), the energy dependence of the capture cross section and the excitation cross section were measured directly.[3] Excitation was found to dominate at the higher bombarding energies ($\gtrsim 30$ MeV). The observed cross-section behavior was indirectly deduced in previous work from total cross-section measurements.[5-8]

In this work we extend these studies to near-symmetric collisions through the study of $F^{q+}+Ne$. It is known in such collision systems that multiple electron loss or gain leads to potentially complicated spectra.[9-13] In spite of this difficulty an attempt is made to elucidate on the charge-state dependences of the processes of single K-shell excitation, single K-shell electron ionization, and L-shell electron capture in nearly symmetric collisions.

II. PROCEDURE

This experiment utilized the facilities of the James R. Macdonald Laboratory, Kansas State University. Negative fluorine ions were extracted from the diode ion source by a 55-kV potential, focused, then momentum analyzed by a 20° inflection magnet. The beam then entered the 6-MV tandem Van de Graaff accelerator. At the terminal of the accelerator, the ions were stripped by passing them through either a thin (5 $\mu g/cm^2$) carbon foil, or a gas stripper canal using oxygen as the stripping gas. The positive fluorine ions were then accelerated out of the machine and momentum analyzed by a 90° magnet with a final energy of 15 MeV. The lower charge states, F^{2+} through F^{5+}, could be selected from the beams following terminal stripping. This method produced currents of from 100 to 300 nA at the Faraday cup. The cross sections for producing the higher charge states, F^{6+} through F^{9+}, are too small to produce usable beams in this manner, therefore a thin (5 $\mu g/cm^2$) carbon post stripping foil was inserted in the beam after the 90° magnet. In this geometry a 15-MeV F^{4+} primary beam could be stripped to the desired charge state. The desired charge state produced by either of the two methods was then chosen by the switching magnet which deflected the beam 45° into the experimental beam line. Using the second method, beam currents of from 2 to 400 nA in charge states 6^+ to 9^+ were obtained in the Faraday cup. The beam was focused by a quadrupole lens, and collimated

by two adjustable four-jaw slits before entering the target chamber. The first four-jaw is used to define the beam size; the second four-jaw is used to clean up beam scattered by the first set of slits.

The target chamber is shown schematically in Fig. 1. The fluorine beam entered the gas cell through the entrance aperture (1.8-mm diameter), and exited the gas cell through the exit aperture (2.0-mm diameter) to be collected by the Faraday cup. The neon target gas was introduced into the interaction region by a single-stage regulator and needle valve arrangement. The gas pressure in the cell was monitored by a Baratron pressure gauge and was constant to within 5% with no further regulation of input flow necessary. The vacuum in the beam line was maintained by a differentially pumped system consisting of three 6-in. oil diffusion pump/mechanical roughing pump stations, which kept the residual pressure in the beam line to between 10^{-6} and 10^{-7} Torr and kept the intermediate region to $\sim 10^{-5}$ Torr. Several spectra were taken with the neon gas valved off to determine the influence of residual gases on the fluorine spectra. This residual background was low enough that no correction to the data was necessary. A fourth pumping station, consisting of a 4-in. oil diffusion pump and mechanical roughing pump, was used to pump the spectrometer chamber.

A problem often encountered in gas target experiments is contamination of the target. Nitrogen, oxygen, and argon contained in the gas cell can significantly alter the x-ray yields of the fluorine ions. These impurities must be monitored in order to ensure the accuracy of the data collected. This was accomplished by mounting a surface barrier detector in the interaction region at 35° to the beam axis. Fluorine ions elastically scattered from the gases in the cell, and the recoil of these gases from the fluorine ion impact were recorded by the detector. A typical spectrum of the particle detector is shown in Fig. 2, along with an energy calibration and the calculated energies of suspected contaminant reaction products.

The x rays produced due to collisions in the gas cell were wavelength analyzed by an Applied Research Laboratories (ARL) curved crystal spectrometer. The front edge of the spectrometer entrance slit is located about 5 mm downstream from the gas cell entrance aperture. The slit was 0.38×12.5 mm^2 in size and was placed parallel to the beam to act as a collimator for the x rays and as a baffle to the target gas. The x rays were reflected by a 4-in. rubidium acid phthalate (RAP) crystal, $2D = 26.121$ Å, into a flow mode proportional

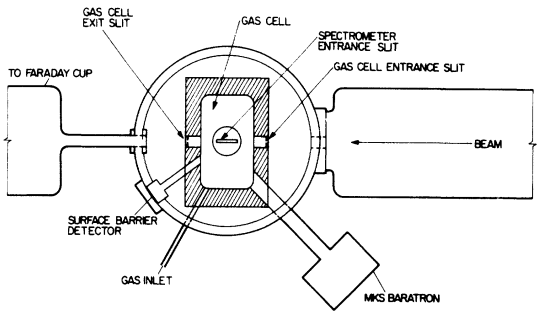

FIG. 1. Schematic of the target chamber showing major features.

counter operated at +2000 V, using a P-10 (90% argon, 10% methane, molar percentage) detector gas mixture at atmospheric pressure contained behind a thin Mylar $(C_{10}H_8O_4)_n$ window.

The data collection and spectrometer control were monitored by an on-line PDP-11 computer. The charge accumulated by the Faraday cup was digitalized by a Brookhaven Instruments Corporation Current Integrator before being input to the computer. This digitalized charge was summed until a preset limit was reached at which time the spectrometer was instructed to move to the next wavelength angle setting. During the spectrometer rota-

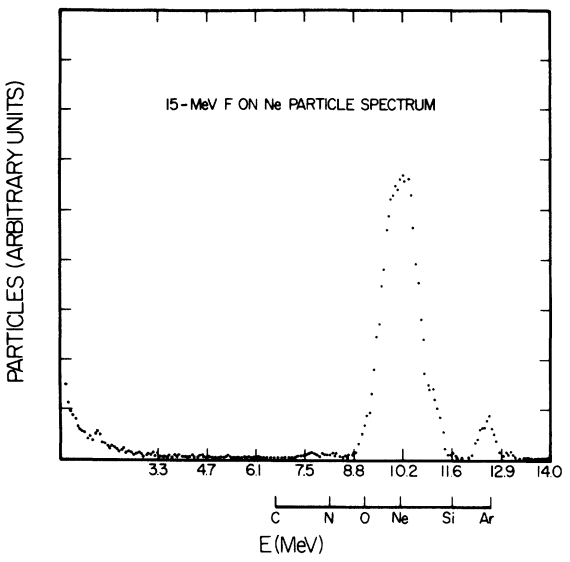

FIG. 2. Typical spectrum from surface barrier detector which viewed the interaction region. The energies of F ions which had scattered from various suspected contaminants as well as the Ne target gas are shown.

tion, the amount of beam integrated was noted so that a dead-time correction could be applied to the recoil monitor spectrum.

A major advantage inherent in the use of a gas target is the ability to minimize the number of incident ions which undergo multiple collisions within the target chamber. Figure 3 gives the results of a pressure-dependence study which shows the yields of various projectile x-ray transitions as a function of the target gas pressure. The yields are shown to be linear with pressure through 40 mTorr after which the effects of multiple collisions become important. All of the remaining data in this work were taken at a pressure of 40 mTorr.

III. RESULTS

Figure 4 shows the relative F K x-ray spectra as a function of the incident fluorine-ion charge state for the F^{2+}, F^{3+}, F^{4+}, F^{5+}, and F^{6+} projectiles on Ne. The K x-ray spectra of F for F^{7+}, F^{8+}, and F^{9+} incident on Ne are given in Fig. 5. The K x rays are identified according to the configuration of the F ion prior to x-ray emission. The multielectron initial states occurring at low energies in the x-ray spectra are labeled according to their configurations "KL^n," such as the KL^4 initial state at 702.3 eV, the KL^3 at 713.0, and the $KL^2(^4P)$ and (^2P) at 714.8 and 725.3 eV, respectively. The energy resolution of the spectrometer, about 4 eV, was not sufficient to distinguish the KL^3 from the $KL^3(^4P)$, so there is some ambiguity as to the relative cross sections in-

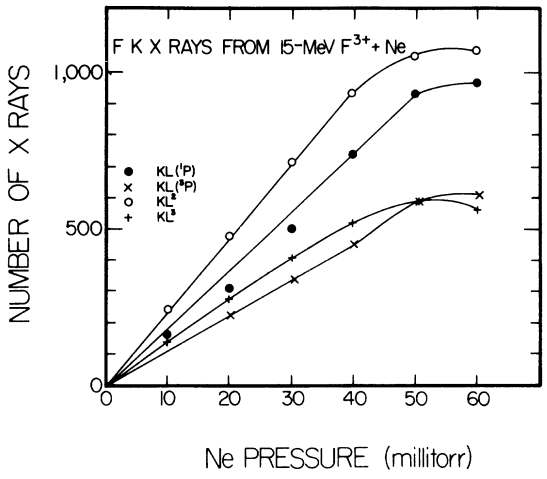

FIG. 3. Dependence of F K x rays vs Ne target pressure. All subsequent data collected for this work were at a pressure of 40 mTorr.

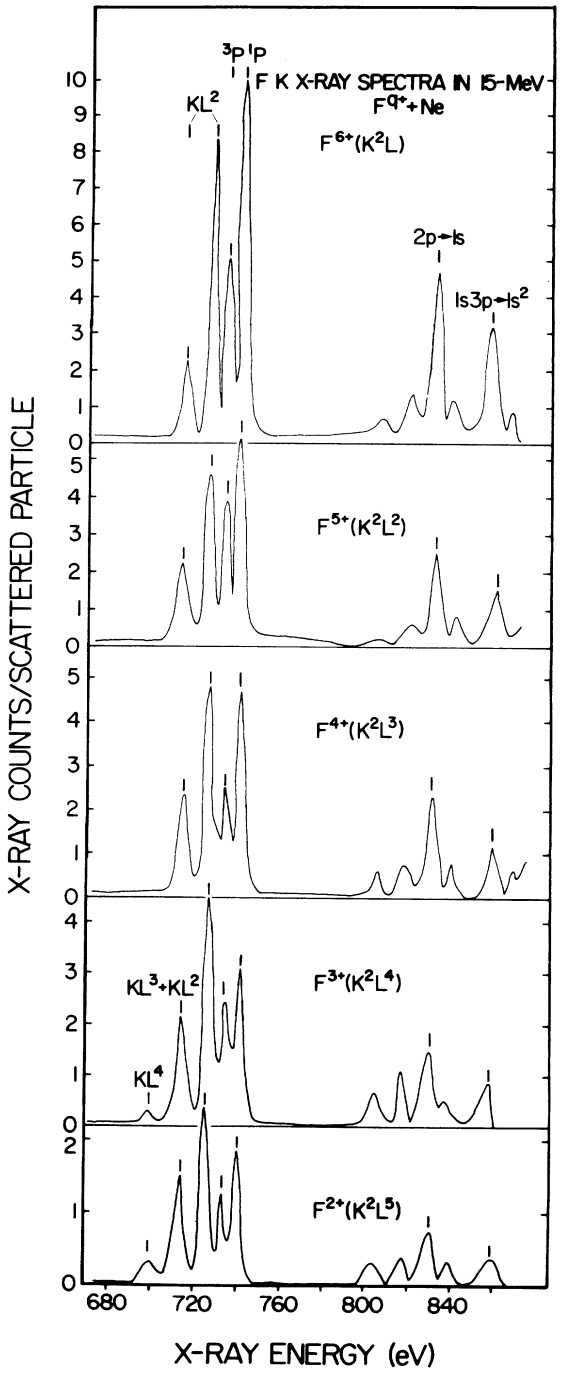

FIG. 4. F K x-ray spectra following a $F^{q+}(q=2\rightarrow6)+Ne$ collision. The spectrometer scan is over an energy range of 680 to 860 eV with a resolution of 4 eV.

volved; however, the ^4P state is metastable with a long lifetime ($\tau=16.2$ nsec), so the majority of ions left in the ^4P configuration will move beyond the acceptance angle of the spectrometer before decay-

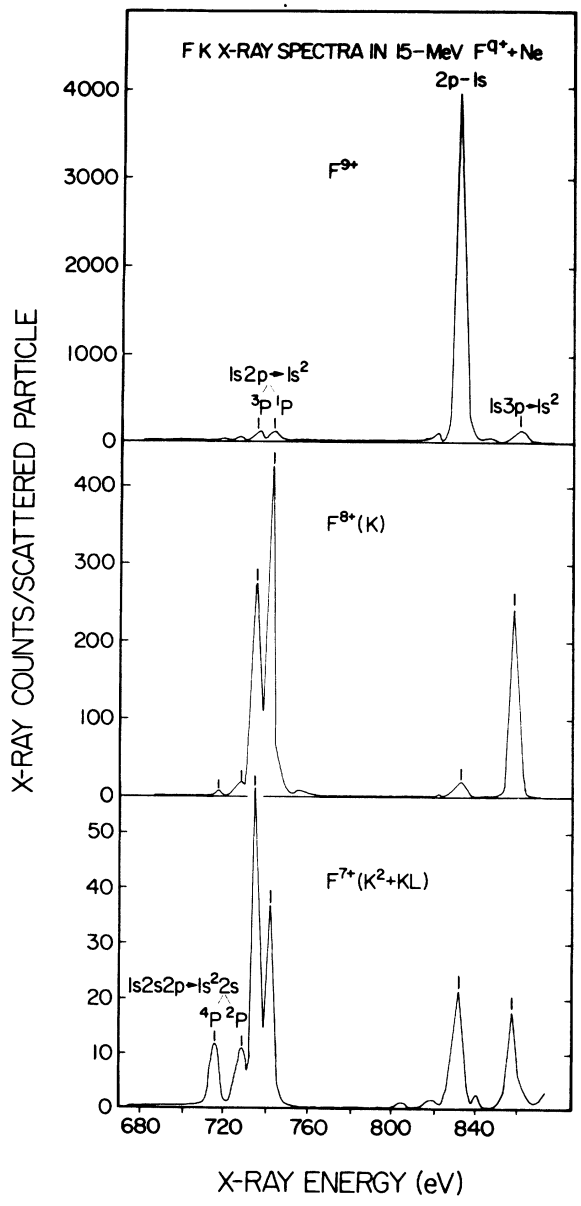

FIG. 5. Spectra for $F^{q+}(q=7\rightarrow 9)+Ne$. The spectrometer scan is over an energy range of 680 to 860 eV with a resolution of 4 eV.

ing. Heliumlike initial states were observed at three energies of the x-ray spectra; at 731 and 737.7 eV transitions occur involving the $1s2p\ ^3P$ and ^1P configurations and at 858 eV the third observed heliumlike transition occurs, coming from the $1s3p$ configuration. The peaks at 803 and 816 eV are not positively identified, but are believed to be due to doubly excited states of heliumlike and lithiumlike systems.

The systematics of the data are readily apparent from Figs. 4 and 5. As the charge state of the incident ion is increased, the cross sections for producing various configurations show a gradual shift toward higher final charge states. The cross sections are also increasing with the change in incident-ion charge state, being gradual between F^{2+} and F^{6+}, then becoming quite pronounced as the projectile K shell opens up, $F^{7+}\rightarrow F^{9+}$.

An experimental difficulty precluded our extending the measurement out to the He and H series limit. Owing to the near symmetry of the projectile and the target, the Ne K x-ray satellite lines overlap with the highly ionized F satellite x rays, making accurate determination of the cross sections for these satellites impossible in this experiment.

An experimental difficulty inherent in any charge-state study of a system is the problem of obtaining pure beams in the ground state of the charge required. Unfortunately, for two beams used in this experiment, the purity is insufficient to guarantee that the contaminant fraction does not seriously affect the results. The F^{7+} beam arrives on target with some fraction (about 25%) of the ions in a $1s2s\ ^3S$ metastable state produced in the poststripper foil. This metastable fraction manifests itself in two places: the $1s2s2p\ ^4P$ state formed by single-electron capture to the $2p$ shell of the metastable component, and the $1s2p\ ^3P$ state formed by Coulomb excitation of the metastable electron configuration, both of which show large increases in their relative yields for a F^{7+} beam. Additional work in this area has been done recently.[14] In traveling from the switching magnet to the target chamber, some fraction of the beam will suffer charge-changing collisions. In most cases this is not a serious source of error since it is estimated that less than 0.5% of the beam arrives on target in anything other than the desired charge state. The capture of an electron to the L shell of a F^{9+} ion is indistinguishable from K to L electron excitation of a F^{8+} ion. If only 0.25% of the incident 8^+ beam were in fact 9^+, that impurity fraction would be responsible for a third (2.0×10^{-19} cm^2) of the reported 8^+ electron excitation cross section (6.0×10^{-19} cm^2). We are not able to accurately measure the beam impurity fraction. Therefore, we will not make any correction to the reported cross sections, but we will increase its uncertainty.

The intraexperiment normalization between different charge states and different scans at each charge state utilized the surface barrier detector which viewed the interaction region. The number of particles scattered into this detector in the energy

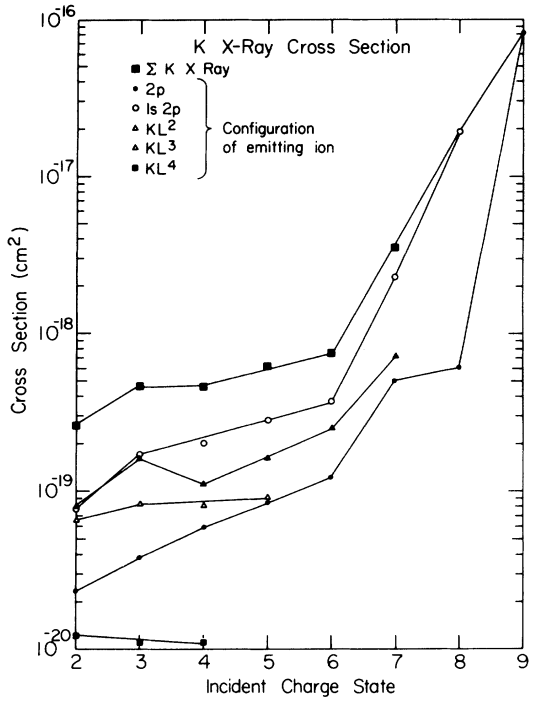

FIG. 6. F K x-ray cross sections following a 15-MeV $F^{q+}(q=2\rightarrow 9)+$Ne collision. The cross sections are plotted vs incident charge state with the various symbols denoting the final charge state.

window selected gave an accurate measure of the product of the number of incident particles times the number of neon atoms contained within the gas cell, a value independent of the ionic charge state since it depends only on nuclear elastic scattering.

After each peak in the spectra had been integrated and background subtracted, the yields thus obtained were corrected for the change in crystal reflectivity and proportional counter window transmission, both of which depend on the x-ray energy. The $1s2p\ ^3P$ state is metastable, so the measured x-ray yield was multiplied by 1.13[4] to correct for the partial decay in flight of that configuration. To normalize these relative yields to absolute cross sections, the data for the 15-MeV F^{3+} incident beam was scaled to the previous work of Woods *et al.*[15] who measured the Auger production cross sections for fluorine on neon. The error in the overall normalization of the cross sections is estimated to be 50%. The relative error is estimated to be 20% for all cross sections except that of F^{8+} electron excitation which could be too large by a factor of 2.0. In Fig. 6 and the upper half of Table I, the fluorine K x-ray cross sections are presented as a function of the incident charge state. The lines in Fig. 6 connect equal final charge states. The sum of all x rays emitted from each incident charge state is shown by the uppermost data points. Tunnell

TABLE I. (a) Measured K x-ray production cross sections, σ_x, for $F^{q+}+$Ne in units of cm^2; and (b) total cross sections $\sigma=\sigma_x/\bar{\omega}$ for $F^{q+}+$Ne in units of cm^2.

	Configuration of emitting ion				
q	KL^4	KL^3	KL^2	KL	L
			(a) σ_x		
2^+	1.2×10^{-20}	6.7×10^{-20}	7.9×10^{-20}	7.7×10^{-20}	2.3×10^{-20}
3^+	1.1×10^{-20}	8.1×10^{-20}	1.6×10^{-19}	1.7×10^{-19}	3.8×10^{-20}
4^+	1.1×10^{-20}	8.1×10^{-20}	1.1×10^{-19}	2.0×10^{-19}	5.9×10^{-20}
5^+		9.1×10^{-20}	1.6×10^{-19}	2.8×10^{-19}	8.4×10^{-20}
6^+			2.5×10^{-19}	3.7×10^{-19}	1.2×10^{-19}
7^+			7.3×10^{-19}	2.3×10^{-18}	4.9×10^{-19}
8^+				1.9×10^{-17}	6.0×10^{-19}
9^+					8.1×10^{-17}
			(b) σ		
2^+	4.4×10^{-19}	9.3×10^{-19}	4.1×10^{-19}	1.4×10^{-19}	2.3×10^{-20}
3^+	4.1×10^{-19}	1.1×10^{-18}	8.3×10^{-19}	3.0×10^{-19}	3.8×10^{-20}
4^+	4.1×10^{-19}	1.1×10^{-18}	7.3×10^{-19}	3.6×10^{-19}	5.9×10^{-20}
5^+		1.3×10^{-18}	8.3×10^{-19}	5.0×10^{-19}	8.4×10^{-20}
6^+			1.3×10^{-18}	6.7×10^{-19}	1.2×10^{-19}
7^+			3.9×10^{-18}	4.1×10^{-18}	4.9×10^{-19}
8^+				3.4×10^{-17}	6.0×10^{-19}
9^+					8.1×10^{-17}

TABLE II. Average configuration *K* x-ray fluorescence yields for F.

Configuration	$\bar{\omega}\times 100$
KL^4	2.68
KL^3	7.18
KL^2	19.2
KL	55.4
L	100

et al.[16] calculated the *K* x-ray fluorescence yields of multiply ionized fluorine, shown in Table II, which were used to obtain the total cross sections for *K*-vacancy production of the lower charge states and capture to excited states of the higher charge states. These data are given in Fig. 7 and in the lower half of Table I.

IV. CONCLUSION

We have used high-resolution x-ray spectroscopy to measure the *K* x-ray production of fluorine ions

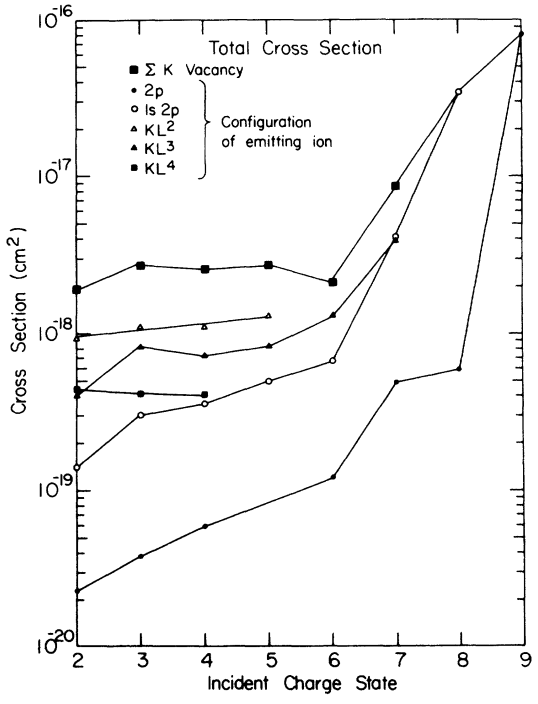

FIG. 7. F total *K*-vacancy-production cross sections following a 15-MeV $F^{q+}(q=2\rightarrow 9)+Ne$ collision. The cross sections are plotted vs incident charge state with the various symbols denoting the final charge state.

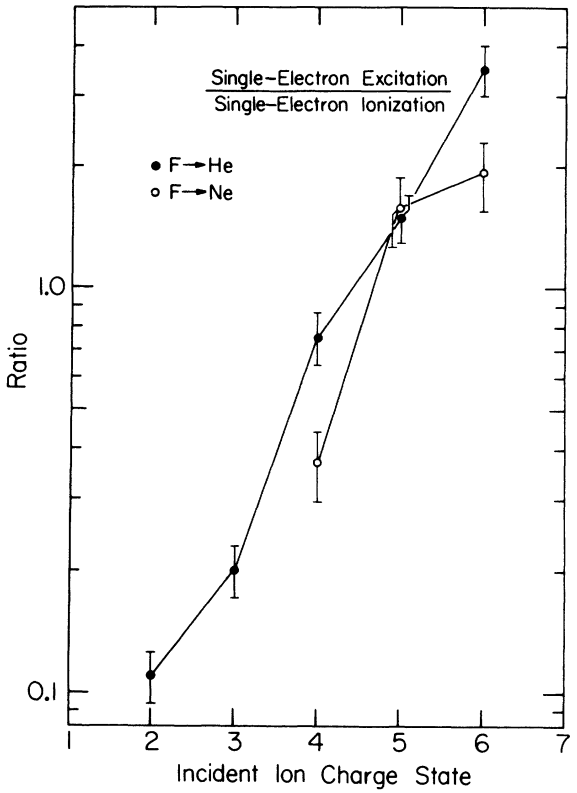

FIG. 8. Ratio of single-electron excitation to single-electron ionization for F^{q+} on He or Ne.

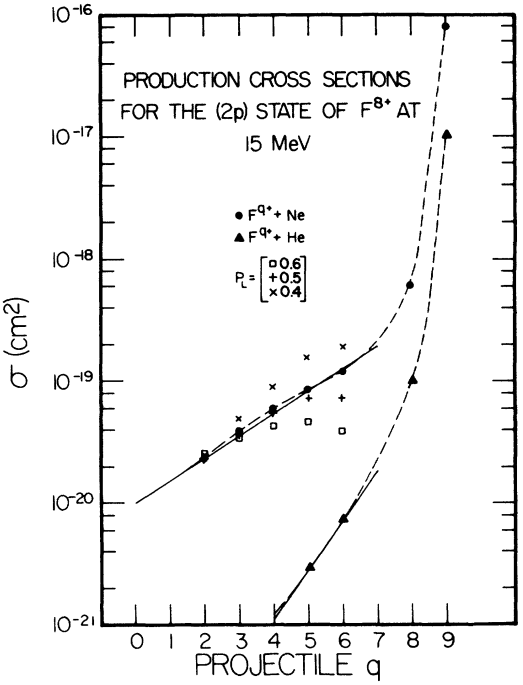

FIG. 9. Cross sections for the production of F^{8+} in the 2*p* state following 15-MeV F^{q+} on He or Ne collisions. The calculations obtained by the binomial expansion model are shown.

after collision with a neon target as a function of the incident ion's charge state. To our knowledge this is the first high-velocity near-symmetric high-resolution projectile x ray versus charge-state study. The cross sections measured by this work point out the relative violence of the near-symmetric K-vacancy-producing collision. We see no single-electron transitions occurring in the lowest charge-state incident beams ($q<4$), while observing the Lyman-α x ray for all incident charge states. However, when the ratio of single-electron excitation to single-electron ionization is plotted as a function of the incident-ion charge state, the slope of the data is remarkably similar to that of the previous work of Tawara *et al.*[4] as shown in Fig. 8. It has been possible to determine from the data the probability for leaving the projectile in the $2p$ state by using a binomial function of the form $A\binom{l}{n}P_L^n(1-P_L)^{l-n}$, where P_L represents the probability of removing one L electron. $\binom{l}{n}$ is the standard binomial coefficient and A is the normalization constant. Using the above equation, it can be shown that the probability of leaving the ion in the hydrogenlike $F^{8+}(2p)$ state for an incident $q+$ projectile is given by

$$(7-q)P_L^{(6-q)}(1-P_L)\ .$$

Figure 9 shows the cross sections for producing the $2p$ state of F^{8+} as a function of incident charge state for F on He,[4] and F on Ne (present work). The predictions of the statistical model are shown by the various symbols for $P_L=0.6$, 0.5, and 0.4. It is seen that the binomial expansion approximates the exponential dependence of the data over a limited range of q for $P_L\simeq 0.5$. The data for the incident 7^+ beam are not plotted due to the ambiguity presented by the metastable portion of the beam. It should be emphasized that this is a statistical model, not a theory. The lack of an applicable theory concerning the charge-state dependence of heavy ion-atom collisions is a subject that requires considerably more attention.

ACKNOWLEDGMENT

This work was supported by the U. S. Department of Energy, Division of Chemical Sciences.

[1]J. R. Macdonald, P. Richard, C. L. Cocke, and I. A. Sellin, Phys. Rev. Lett. 31, 684 (1973).
[2]F. F. Hopkins, Robert L. Kauffman, C. W. Woods, and Patrick Richard, Phys. Rev. A 9, 2413 (1974).
[3]H. Tawara, Patrick Richard, K. A. Jamison, and Tom J. Gray, J. Phys. B 11, L615 (1978).
[4]H. Tawara, Patrick Richard, K. A. Jamison, Tom J. Gray, J. Newcomb, and C. Schmiedekamp, Phys. Rev. A 19, 1960 (1979).
[5]F. F. Hopkins, Andrew Little, and Nelson Cue, Phys. Rev. A 14, 1634 (1976).
[6]J. A. Guffey, Ph.D dissertation, Kansas State University, 1977 (unpublished).
[7]U. Schiebel, B. L. Doyle, J. R. Macdonald, and L. D. Ellsworth, Phys. Rev. A 16, 1089 (1977).
[8]B. L. Doyle, U. Schiebel, J. R. Macdonald, and L. D. Ellsworth, Phys. Rev. A 17, 523 (1978).
[9]A. R. Knudson, D. J. Nagel, and P. G. Burkhalter, Phys. Lett. 42A, 69 (1972).
[10]D. Burch, P. Richard, and R. L. Blake, Phys. Rev. Lett. 26, 1355 (1971).
[11]R. L. Watson, A. K. Leeper, B. I. Sonobe, T. Chiao, and F. E. Jenson, Phys. Rev. A 15, 914 (1977).
[12]C. F. Moore, D. L. Matthews, and H. H. Wolter, Phys. Lett. 54A, 407 (1975).
[13]C. Schmiedekamp, B. L. Doyle, T. J. Gray, R. K. Gardner, K. A. Jamison, and P. Richard, Phys. Rev. A 18, 1892 (1978).
[14]M. Terasawa, Tom J. Gray, S. Hagmann, J. Hall, J. Newcomb, P. Pepmiller, and Patrick Richard, Phys. Rev. A (in press).
[15]C. W. Woods, R. L. Kauffman, K. A. Jamison, N. Stolterfoht, and P. Richard, Phys. Rev. A 13, 1358 (1976).
[16]T. W. Tunnell, C. Can, and C. P. Bhalla, IEEE Trans. Nucl. Sci. NS-26, 1124 (1979).